

NRC Publications Archive Archives des publications du CNRC

Control over strain in the dynamic modulus test

Osman, A.; ElHussein H Mohamed, xxx; Adam, Y.; Zeghal, M.; Maadani, O.

This publication could be one of several versions: author's original, accepted manuscript or the publisher's version. /
La version de cette publication peut être l'une des suivantes : la version prépublication de l'auteur, la version
acceptée du manuscrit ou la version de l'éditeur.

Publisher's version / Version de l'éditeur:

*Transportation Research Board 86th Annual Meeting [Proceedings], pp. 1-25,
2007-01-21*

NRC Publications Archive Record / Notice des Archives des publications du CNRC :

<https://nrc-publications.canada.ca/eng/view/object/?id=6c3581f7-c59d-4b34-931c-16044e9bef45>

<https://publications-cnrc.canada.ca/fra/voir/objet/?id=6c3581f7-c59d-4b34-931c-16044e9bef45>

Access and use of this website and the material on it are subject to the Terms and Conditions set forth at

<https://nrc-publications.canada.ca/eng/copyright>

READ THESE TERMS AND CONDITIONS CAREFULLY BEFORE USING THIS WEBSITE.

L'accès à ce site Web et l'utilisation de son contenu sont assujettis aux conditions présentées dans le site

<https://publications-cnrc.canada.ca/fra/droits>

LISEZ CES CONDITIONS ATTENTIVEMENT AVANT D'UTILISER CE SITE WEB.

Questions? Contact the NRC Publications Archive team at

PublicationsArchive-ArchivesPublications@nrc-cnrc.gc.ca. If you wish to email the authors directly, please see the
first page of the publication for their contact information.

Vous avez des questions? Nous pouvons vous aider. Pour communiquer directement avec un auteur, consultez la
première page de la revue dans laquelle son article a été publié afin de trouver ses coordonnées. Si vous n'arrivez
pas à les repérer, communiquez avec nous à PublicationsArchive-ArchivesPublications@nrc-cnrc.gc.ca.



<http://irc.nrc-cnrc.gc.ca>

Control over strain in the dynamic modulus test

NRCC-48706

Ali, O.; ElHussein H. Mohamed; Adam, Y.;
Zeghal, M.; Maadani, O.

A version of this document is published in
/ Une version de ce document se trouve
dans: Transportation Research Board 86th
Annual Meeting, Washington, D.C., Jan.
21-25, 2007, pp. 1-25



National Research
Council Canada

Conseil national
de recherches Canada

Canada

CONTROL OVER STRAIN IN THE DYNAMIC MODULUS TEST

Submission Date: November 15th 2006

Abstract: 258; word Count: 7200 (Text: 3950; Tables and Figures: 13)

By

Osman Ali (Corresponding author)

Institute for Research in Construction, National Research Council Canada

1200 Montreal Road, M-20

Ottawa, Ontario K1A 0R6 Canada

Phone: (613) 993-0127

Fax: (613) 954-5984

Email: osmans2@hotmail.com

ElHussein H. Mohamed

Institute for Research in Construction, National Research Council Canada

1200 Montreal Road, M-20

Ottawa, Ontario K1A 0R6 Canada

Phone: (613) 993-3817

Fax: (613) 954-5984

Email: Elhussein.h.Mohamed@nrc-cnrc.gc.ca

Yassin Adam

Graduate Student, Civil Engineering Department

1125 Colonel By Drive

Carleton University

Ottawa, Ontario K1S 5B6

Phone: (613) 520-7400

Canada

Morched Zeghal

Institute for Research in Construction, National Research Council Canada

1200 Montreal Road, M-20

Ottawa, Ontario K1A 0R6 Canada

Phone: (613) 991-6237

Fax: (613) 954-5984

Email: Morched.zeghal@nrc-cnrc.gc.ca

Paper Prepared for Presentation at the 2007 Annual Meeting of the Transportation Research Board

CONTROL OVER STRAIN IN THE DYNAMIC MODULUS TEST

ABSTRACT

Bituminous mixtures exhibit complex visco-plasto-elastic behavior. However, implementation of purely linear viscoelastic properties at this early stage in the implementation of mechanistic-based models used in the analysis of flexible pavements is a reasonable starting point. This simplifying assumption requires that testing of asphalt concrete be performed at low strain amplitudes where the material response remains linear visco-elastic. The material testing system included in the NCHRP 1- 37A project adopted the dynamic modulus as the input to the M-E model that accounts for HMA stiffness, a property necessary for performing structural analysis to determine the state of stresses and strains in the asphalt concrete layer. The model uses the established state of stresses and strains to predict rutting and fatigue and other distress types using performance models incorporated in the software.

The current dynamic modulus testing approach is based on AASHTO standard test specifications designated TP62-03. This paper examined the response of a variety of HMA mixes using an alternative dynamic modulus testing technique based on controlling the strain in order to make sure that the linear viscoelastic assumption is truly being respected under the proposed stress-controlled testing technique. Results obtained using the strain-controlled testing technique suggest that the levels of stress proposed under TP62-03 are relatively high and may expose the material to a critical condition exceeding the viscoelastic response and leading to accumulation of permanent deformations. The strain-controlled testing approach seems to offer a more practical and reliable technique for determining the dynamic modulus of asphalt concrete mixes needed as input to the new M-E design model.

Key Words: HMA; dynamic modulus; strain- controlled; NCHRP 1-37A; viscoelastic response

BACKGROUND

Effective characterization of construction materials is a key requirement for successful pavement analysis and design. Characterization should be based on material properties that accurately capture the material response to external stimuli associated with traffic loading as influenced by construction quality and environmental conditions. At this early stage in the implementation of mechanistic-based models, the dynamic modulus is gaining popularity because of its ability to quantify the stiffness of asphalt concrete as affected by mix type, temperature condition and rate of loading. In the M-E pavement design guide developed under NCHRP project 1-37A, the process of obtaining a value for the dynamic modulus differs from one input level to another (1). At input level 1, the dynamic modulus is determined directly in the laboratory at different temperatures and loading frequencies according to AASHTO provisional standard testing procedure designated TP62-03 (2). At input level 3, the complex modulus test is not required and the modulus could be estimated using a predictive equation.

Early attempts to capture the viscoelastic response of HMA involved the use of the complex modulus testing approach with traffic loading simulated in the laboratory with a sinusoidal load. The obtained material response is also sinusoidal in nature but with a phase lag (3, 4, 5, 6). Sinusoidal loading is performed at different frequencies within the linear viscoelastic range. According to the theoretical construct of the complex modulus approach, loading could be performed under either a stress or strain-controlled mode. In the first case, a specific stress value is applied and the corresponding strain is obtained, while in the other case, specific strain amplitude is applied and the corresponding stress is recorded.

Stress-Controlled Test

The dynamic modulus is the only component of the complex modulus that has been implemented in the new M-E pavement design guide. The structural response model is based on linear elasticity, and hence, the phase angle is not being considered in the analysis. Future development in mechanics may make it possible to incorporate the effect of the phase angle in the structural response model. The AASHTO provisional test standard TP62-03 is performed at temperatures of -10, 4.4, 21.1, 37.8 and 54.4 °C. Frequencies of 25, 10, 5, 1, 0.5 and 0.1 Hz are specified for loading the sample at each temperature. The recommended protocol is a stress-controlled version of the complex modulus test in which the sinusoidal (haversine) cyclic load applied to the specimen is adjusted so that the specimen is subjected to axial strains between 50 and 150 microstrain ($\mu\epsilon$). This constraint is in place to guarantee that testing is being performed within the linear viscoelastic zone. According to the current test protocol, the stress level should be selected from a certain range set for each test temperature. Recommended stresses are included in Table 4 of AASHTO test specifications TP62-03 (2), which range from 35 to 2800 kPa (5 to 400 psi). However, the dynamic loads that achieve the targeted strain magnitude depend on the HMA mix stiffness. Accordingly, experience with the dynamic modulus test procedure and the HMA mixes being tested is critical for proper selection of the stress level that complies with the strain limitation (7). Relatively high loads are needed at colder temperatures and smaller loads at warmer temperatures to keep axial strain within the linear zone. Additional measures are proposed to manage the strain level during the test. It is recommended to observe the strain at the end of any testing series at

each test temperature and to act by reducing the maximum loading stress level by half if the cumulative un-recoverable permanent strain is found to be greater than 1500 micro units of strain. As a result of this precaution, it is expected that many specimens will be discarded and new ones used for the rest of testing periods under the reduced load condition. This paper discusses a practical alternative testing approach for controlling the strain in order to guard against violating the assumption that the material is within the linear viscoelastic state when the dynamic modulus is determined.

Strain-Controlled Test

In a pavement structure, traffic induces stresses within the HMA layer and as a result, strains develop suggesting that the laboratory test should follow a stress-controlled mode to mimic this field-loading pattern. However, previous work performed under the stress-controlled mode has experienced difficulties in limiting displacements within the desired range, i.e., below what may cause permanent strain. In the literature, a strain magnitude of 1500 $\mu\epsilon$ has been reported at test temperatures between 40 and 50°C (8). Practicality of the strain-controlled testing approach motivated European researchers to experiment with this technique. Heck et al. (3) performed successfully the classical French alternate flexural test on trapezoidal specimens under sinusoidal strain for the crossed frequency-temperature conditions: [1, 3, 10, 30, 40 Hz] \times [-10, 0, 10, 20, 30, 40°C]. Bonnaure et al. (9) determined the complex modulus of asphalt mixtures from bending tests using a trapezoidal specimen fixed at one end and subjected to a sinusoidal load at the free end. Witczak and Root indicated that a tension-compression test might be more representative of field loading conditions (10). After performing the complex modulus tests under five different modes of loading, Khanal and Mamlouk confirmed the findings of Witczak and Root (11). Accordingly, cyclic loading in this study was performed using tension-compression to produce the data necessary for calculating the dynamic modulus.

EXPERIMENTAL INVESTIGATION

The laboratory investigation designed to investigate the effectiveness of the strain-controlled alternative proposed in this study included some features of the stress-controlled approach for determining the modulus needed as input to the NCHRP 1-37A model. Loading of the specimen was conducted at the frequencies of 20, 10, 5, 1, 0.3 and 0.1 Hz at each test temperature (-10, 0, 10, 20, 30, and 40°C). Samples that represent three types of conventional hot mix asphalt (HMA 1, 2 and 3) designed using the Marshall approach and two according to Superpave volumetric mix design (SP1, SP2) using AASHTO provisional specifications (MP2-02), were prepared as shown in Table 1. The function of these five mixes conforms to a wide range of applications; mainly binder and surface courses. A gyratory compactor was used to prepare the specimens with a tolerance for air voids set at 0.5 %. Mechanical tests were performed on samples after an age of six days and a minimum of two replicates were used in each test.

Tension-compression complex modulus tests were performed on the two mix types under the strain-controlled approach using the National Research Council Canada (NRCC) standard specification WI # 440500-9328-4.9I-UIR85 (12). A servo-hydraulic testing system (MTS810, Teststar II frame) furnished with MultiPurpose Testware was used to control the cyclic load applied to HMA samples as shown in Figure 1. An environmental chamber capable of controlling the temperature over the desired range

within ± 0.5 °C was used for conditioning samples. Axial deformations were measured using extensometers with high accuracy (MTS product Model 632.11F-90). The extensometers were mounted on the side of the specimen at 180° apart and attached to the specimen by springs and their knife-edges were glued using a drop of five-minute epoxy. Platens used to transmit the load to the specimen were glued to the two ends of the specimens. In loading the specimen, a short rest period of two minutes was assigned after 20 and 10 Hz for testing at temperatures of -10 , 0 , and 10 °C. A rest period of one minute was assigned after 5, 1, 0.3, and 0.1 Hz for tests performed at -10 , 0 , and 10 °C. Also a rest period of one minute was assigned after all frequencies for testing at temperatures of 20 , 30 , and 40 °C. The adopted sampling rate was 100 points per cycle, which was found to be adequate for accurately plotting sinusoidal signals capturing effectively peak stress and strain values (13). The commercial statistical package entitled TableCurve was used to reduce data and fit it to a waveform equation (sinusoidal) to assist in determining amplitudes of the stress and strain signals and the phase angle. The software HUSAROAD, a module of the VEROAD Program (14), was used to construct master curves that depict variations in the stiffness with temperature for mixes tested in this study.

RESULTS AND ANALYSIS

Results from preliminary strain-controlled tests performed in this study were instrumental in the test procedure refinement task. One such exercise involved determination of the number of loading cycles in the strain-controlled test. The objective was to achieve a strain output signal equivalent to the input value. The number of cycles recommended in the AASHTO test protocol was used initially in the strain-controlled test only to discover that the output signal of the strain at the end of the recommended number of load cycles remained lower than the input value. The number of cycles differed according to loading frequency and test temperature for each of the tested HMA type. Higher numbers were needed for the output strain value to reach the input value as shown in Figure 2.a. Initially the testing system attempts to comply with the displacement control requirement issued by a signal from the extensometers attached to the sample. These initial attempts are usually not adequate for compliance of the system which seems to be influenced by the nature of the material being tested, loading frequency, temperature and stiffness of the loading frame. The system continues attempts to produce the actuator movement that will push the specimen up to the targeted displacement value and the load cell captures the corresponding load signal. The extensometer then records the actual displacement of the sample corresponding to the recorded load (see Figure 2.b). This process continues until the output strain is equivalent to the input. When compliance is achieved, after the adequate conditioning cycles, an Excel macro records data corresponding to the last three cycles. This number is also different from what has been recommended in the TP62-03 protocol which calls for recording data from the last five cycles. It is worth noting that regardless of the number cycles used to collect test data, it is important to make sure that the system achieves compliance with the specified strain magnitude after which other corresponding outputs (stress and phase angle) could be accurately determined. Using data from the last five cycles that follows conditioning cycles specified in the current TP62-03 protocol will not necessarily yield accurate data output for effective determination of the dynamic modulus.

At a temperature of -10°C and a loading frequency of 20 Hz, 1000 cycles were needed to reach the targeted strain value used to control the loading. The number of cycles required to achieve compliance of the system at cold temperatures was greater than the number of cycles required at warm temperatures. Moreover, more cycles were required to reach the stabilization state at high loading frequencies than at low frequencies. Table 2 shows the number of cycles used in the stress-controlled test specified in AASHTO TP62-03 (2) together with those obtained in the strain-controlled test specified in the NRCC test protocol produced by this study.

Strain Magnitude

The displacement magnitude that could be used effectively in the strain-controlled test was investigated using a linearity check. The objective of the linearity check was to select a maximum displacement to apply without violating the linear viscoelastic state. Considering the possibility of energy loss at different joints and connections within the test setup, small displacements may lead to smaller signals that are hard to process making it difficult to properly and accurately measure the targeted response. The linearity checks were initially performed on the SP 2 mix (Superpave mix, binder PG 52-34) using nine different strains in conducting the complex modulus test. Results from the nine tests, collected at a temperature of 25°C and a loading frequency of 20 Hz, are shown in Figure 3. Stresses corresponding to each of the nine strain values were plotted in Figure 3 to facilitate identification of the transition zone from linear to non-linear response. It is clear from Figure 3 that beyond a stress level of 200 kPa the material acquired permanent deformation and consequently, a strain magnitude of about $100\text{ }\mu\epsilon$ has been considered as the proper value to use in conducting the strain-controlled tests.

The choice of a strain value for conducting the test was reevaluated by performing the linearity check on the HMA 2 mix prepared with a PG 64-34 binder. Results of seven tests performed at different strain values, obtained at $+10$ and $+25^{\circ}\text{C}$ covering all six frequencies (20, 10, 5, 1, 0.3 and 0.1 Hz), are shown in Figure 4. Results obtained at $+10^{\circ}\text{C}$, shown in Figure 4, suggest that the dynamic modulus at each frequency remained unchanged up to a strain level of $100\text{ }\mu\epsilon$ supporting the choice made using the SP 2 mix. Figure 4 also shows results of the linearity checks performed at a relatively warmer temperature ($+25^{\circ}\text{C}$). Linearity was adequately maintained until the strain exceeded $100\text{ }\mu\epsilon$. The strain limit determined in this study is in agreement with earlier findings by Charif (15) but still ten fold higher than that determined by Doubbaneh (16). Based on the above analysis, strain amplitude of $100\text{ }\mu\epsilon$ was selected for conducting all complex modulus tests in this study designed for determining the dynamic modulus.

Stress vs. Strain-Controlled

Results of the complex modulus tests performed using the strain-controlled mode were used to evaluate corresponding stresses associated with the application of $100\text{ }\mu\epsilon$. These stresses were then compared with the levels recommended in the AASHTO TP62-03. The stresses obtained from all the strain-controlled experiments are shown in Table 3 covering ten mixes. In general, the lower stress value proposed in the AASHTO TP62-03 seems reasonable especially at low-test temperatures. Analysis also indicates that at relatively warm temperatures and for some mixes prepared with soft binders, the lower stress value is high. Even with the provision included in the AASHTO TP62-03 that

recommends the use of half the proposed stress in the event that permanent deformation starts to accumulate, the linear viscoelasticity assumption would have been violated as a result of applying such high stresses. Data collected at -10 and 40°C was plotted in Figure 5. At -10°C, the AASHTO TP62-03 proposed stresses are high for four of the mixes evaluated in this study. The stress determined using the train-controlled approach for the fine mix prepared with a neat binder (HMA 3, PG 58-22) is in agreement with the proposed AASHTO limits. However, for the two mixes prepared using modified binders as well as the coarse mixes (HMA 1), the 1400 kPa stress level proposed in AASHTO TP62-03 will be high for tests performed at low loading frequencies (lower than 5 Hz). The proposed lower stress limit was 2.5 times higher than what is needed to produce 100µε; the safe limit set for maintaining the response within the viscoelastic zone. It is worth noticing that the stress level required to achieve 100µε in the case of the fine mix (HMA 3) prepared with modified binders (PG 64-34 or 52-34) was half that required in the mix prepared with a neat binder (HMA 3, PG 58-22).

Figure 5 also compares stresses produced in the controlled-strain test with AASHTO proposed limits at 40°C. It is clear that applying the proposed limits will lead to violation of the viscoelastic assumption in all tested mixes. The proposed lower stress limit was three to six times higher than the stress magnitude required for producing 100µε, especially at low loading frequencies. Further analysis was performed using the Superpave mix (SP 1) and the results were consistent with observation made in the case of Marshall mixes. These results suggest that caution should be exercised when testing mixes with modified binders since the stress required for maintaining the 100µε is much lower than that needed for testing mixes prepared with neat binders as shown in Figure 6. Considering the fact that the proposed stress was 6 times higher than that required to produce 100µε (350 kPa compared with 50 kPa determined in the strain-controlled test), using half the lower limit will not serve as an adequate measure.

Dynamic Modulus

Concerns discussed in this paper associated with uncertainties about the appropriate stress level to use in the stress-controlled testing technique, motivated authors to recommend the use of the strain-controlled approach. Complex modulus data collected from tests performed in this study using the strain-controlled approach was processed to determine the dynamic modulus $|E^*|$ and phase angle ϕ according to Equations 1 and 4 respectively. Raw data recorded during the complex modulus test included records of forces detected by the load cell following a real time sequence (seconds). These are the forces associated with applied displacements controlled by the extensometer. The tests performed at each temperature and loading frequency involves more than 5000 data points needed to draw the full stress-strain profile. The data was processed in the first stage using an Excel-based macro, which involved calculating the stress (Equation 2) and the strain (Equation 3) from the last three cycles of each frequency.

$$|E^*| = \frac{\sigma_0}{\varepsilon_0} \dots\dots\dots 1$$

$$\sigma_0 = \frac{P}{A} \dots\dots\dots 2$$

where A is the cross-sectional area (mm^2) of a specimen with 100-mm diameter, and P is the recorded axial force, (Newton).

$$\varepsilon_0 = \frac{\Delta}{L} \dots\dots\dots 3$$

where Δ is the measured displacement in mm, and L is the gauge length of the extensometer used to control the test

$$\phi = (\phi_1 - \phi_2) * 180/\pi \dots\dots\dots 4$$

where ϕ_1 and ϕ_2 are individual phase angles of the stress and strain wave functions respectively.

The statistical package “TableCurve” was used to obtain amplitudes of stresses and strains in addition to the phase angle of each stress and strain signal for the entire sweep of test temperatures and loading frequencies. The “TableCurve” quantifies the amplitudes of stresses and strains in addition to the phase angle of each stress and strain signal mathematically in terms of the coefficients shown in Equations 5 and 6:

$$\sigma = a_1 + b_1 \sin(2\pi t/d_1 + c_1) \dots\dots\dots 5$$

$$\varepsilon = a_2 + b_2 \sin(2\pi t/d_2 + c_2) \dots\dots\dots 6$$

where: σ and ε are the stress and strain respectively at time t ,

b_1 and b_2 represent the amplitude of stress and strain σ_o and ε_o respectively,

a_1 and a_2 are regression constants,

c_1 and c_2 represent individual phase angles of stress and strain wave functions ϕ_1 and ϕ_2 respectively.

The statistical output of the TableCurve for a typical strain computation is shown in Table 4 reflecting accuracy associated with fitting the data to a sinusoidal waveform function that reflects the material response to applied loading.

In the last stage, processing of data involves using the output of the previous stage to calculate the dynamic modulus $|E^*|$ using Equation 1 and the phase lag ϕ using Equation 4. The phase lag between applied stress and corresponding strain signals was calculated as the difference between ϕ_1 and ϕ_2 in radians. The phase lag in radians was then converted into phase angle in degrees according to Equation 2.

Typical dynamic modulus and phase angle data calculated using results of the strain-controlled testing technique and reduced according to the above procedure for the HMA 1 mix prepared with a PG 58-22, are shown in Table 5. These results reflect a consistent picture and the sensitivity of the determined dynamic modulus to variations in temperature and load frequency. Further analysis was performed using the obtained dynamic modulus to reflect its sensitivity to binder types used in the HMA mix. The dynamic modulus profile shown in Figure 7 discriminates effectively between the two HMA 3 mixes prepared with uniquely different binder types (PG 64-34 and PG 58-22). The response associated with the engineered binder (PG 64-34) compared with the neat one (PG58-22) suggests that the objectives of the binder designer aimed at reducing HMA brittleness at low temperatures to minimize cracking, are fulfilled. The measured

dynamic modulus of the HMA 3 mix prepared with a PG 64-34 binder was half that prepared with a PG 58-22 binder. However, both binders produced relatively close dynamic modulus values at relatively high temperatures reinforcing the role played by the aggregate skeleton at such a condition.

Since the new M-E pavement model rely on a master curve produced by manipulating the dynamic modulus test data, the master curves for 13 mixes tested in this study were constructed using the principle of time-temperature superposition. The master curves for these different mixes are shown in Figure 8.

CONCLUSIONS AND RECOMMENDATIONS

- This study investigated stress levels recommended in AASHTO TP62-03, the stress-controlled testing procedure used for the determination of the dynamic modulus of HMA. The recommended ranges were found to be high for tests performed at relatively warm temperatures and low loading frequencies. Using these levels may result in violating the adopted linear viscoelastic assumption.
- Controlling the strain proved to be a more practical approach and eliminates uncertainties associated with the selection of an appropriate stress level. Accordingly, a strain-controlled testing technique was developed using a compression-tension loading mode. The strain-control test offers a reliable process for determining the dynamic modulus.
- Thirteen mixes were tested in this study using the strain-controlled approach and results were successfully used to determine the dynamic modulus. The process is consistent and the determined modulus proven sensitive to factors such mix type, temperature and loading frequency. The determined modulus discriminates effectively between responses of different mix types prepared with different binders.

REFERENCES

1. NCHRP project 1-37A. Development of the 2002 Guide for the Design of New and Rehabilitated Pavement Structures: Phase II. TRB, National Research Council, Washington, D.C. www.trb.org/mepdg/. Accessed January 2005.
2. AASHTO. Standard Method of Test For Determining Dynamic Modulus of Hot-Mix Asphalt Concrete Mixtures. TP62-03.
3. Heck, J. V., Piau, J. m., Gramsammer, J. C., Kerzreho, J. P. and Odeon, H. Thermo- Visco- Elastic Modelling of Pavements Behaviour and comparison with Experimental Data from LCPC Test Track. 5th International Conference on the Bearing capacity of Roads and Airfields, 1998.
4. Kim, Y. R., Seo, Y., King, M., Momen, M. Dynamic Modulus Testing of Asphalt Concrete in Indirect Tension Mode. Transportation Research Record No. 1891, TRB, National Research Council, Washington, D.C., 2004, pp.163-173.
5. Ferry, J. D. Visco-elastic properties of polymers. 3rd Edition. Wiley, N.Y., 1980.
6. Sayegh, G. Viscoelastic properties of bituminous mixtures. Proceedings of the 2nd International conference on structural design of asphalt pavement, pp. 743-755.
7. Dougan, C. E., Stephens, J. E., Mahoney, J., Hansen, G. E*- Dynamic Modulus Test Protocol – Problems and Solutions. Connecticut Department of Transportation. Report Number CT-SPR-0003084-F-03-3, 2003.

8. Timothy R. C., Xingjun L., Mihai O. M., Eugene L. S. Dynamic and Resilient Modulus of Mn/DOT Asphalt Mixtures. Department of Civil Engineering – University of Minnesota. Report submitted to Minnesota Department of Transportation. 2003.
9. Bonnaure, F., Gest, G., Gravios, A., and Uge, P. A New Method of Predicting the Stiffness of Asphalt Paving Mixtures. Proceedings of Association of Asphalt Paving technologists, Vol. 46, 1977, pp. 64-100.
10. Witczak M.W., and Root. R. E. Summary of Complex Modulus Laboratory Test Procedures and Results. American Society for Testing Materials, ASTM Special Technical Publication, Vol. 561, 1974, pp. 67- 94.
11. Khanal, P. P. and Mamlouk M. S. Tensile Versus Compressive Moduli of Asphalt Concrete. Transportation Research Record 1492, 1995, pp.144-150.
12. National Research Council Canada. Complex Modulus Test Protocol And Procedure for Determining Huet–Sayegh Model Parameters. WI # 440500-9328-4.91-UIR85, 2004.
13. Yassin E. A. Asphalt Concrete Characterization Using the Complex Modulus Technique. Thesis submitted in partial fulfillment of the requirements for the degree of Masters of Applied Science in Civil Engineering, Carleton University, 2005.
14. Hopman, P.C. VEROAD. A. Viscoelastic Multilayer Program. 75th TRB meeting, Transportation Research Record 1539, Washington D.C. USA, 1996, pp. 72-80.
15. Charif, K. Contribution à l'étude du comportement mécanique du béton bitumineux en petites et grandes déformations. Thèse de Doctorat: Ecole Centrale Paris, Janvier 1991. 277 p.
16. Doubbaneh, E. Comportement mécanique des enrobés bitumineux des petites aux grandes déformations. Thèse de Doctorat: Institut National des Sciences Appliquées de Lyon, Octobre 1995. 219 p.

TABLES & FIGURES

LIST OF TABLES

- TABLE 1 Mix Design Information
TABLE 2 Number of Loading Cycles
TABLE 3 Stresses (kPa) Corresponding to $100\mu\epsilon$
TABLE 4 Typical Strain Amplitude Produced by “TableCurve”
TABLE 5 Dynamic Modulus (MPa) and Phase Angle ($^{\circ}$) Determined at Different Loading Frequencies and Test Temperatures for HMA1 Mix (PG 58-22)

LIST OF FIGURES

- FIGURE 1 Strain-controlled test setup.
FIGURE 2 Output of the strain-controlled test.
FIGURE 3 Typical stress-strain relationship at a temperature of 25°C and loading frequency of 20 Hz for SP 2 (PG 52-34).
FIGURE 4 Results of a typical linearity check for tests performed at 10°C and 25°C on HMA 2 (PG 64-34).
FIGURE 5 Stresses corresponding to $100\mu\epsilon$ for tests performed at -10°C and 40°C .
FIGURE 6 Stresses corresponding to $100\mu\epsilon$ for tests performed at 20°C .
FIGURE 7 Dynamic modulus determined for HMA 3 reflecting the impact of binder type.
FIGURE 8 Master curves established for all mixes investigated in this study.

TABLE 1 Mix Design Information

Mix Type	Mix Design Parameter	Local Specifications	Test Results		
			PG 58-22	PG 52-34	PG 64-34
HMA 1 <i>Stabilized Base Course</i>	Asphalt Content %	4.5 - 7.0	4.5	4.5	
	Air Voids %	3 - 5	4.2	4.0	
	Marshall Stability (N)	8000 (min)	11550	9220	
	Marshall Flow (0.25 mm) @ 3.5% Air Voids	8.0 (min)	10.2	8.4	
	VMA %	12.5 (min)	13.85	13.6	
HMA 2 <i>Binder Course</i>	Asphalt Content %	5.0 - 7.0	5.0	5.0	5.1
	% Air Voids	3 - 5	4.6	4.4	4.5
	Marshall Stability (N)	8900 (min)	19200	11800	19000
	Marshall Flow (0.25 mm) @ 3.5% Air Voids	8.0 (min)	11.5	11	11.75
	VMA %	13.0 (min)	13.38	13.04	13.2
HMA 3 <i>Surface Course</i>	Asphalt Content %	5.0 - 7.0	5.0	5.0	5.0
	% Air Voids	3 - 5	4.5	4.5	4.4
	Marshall Stability (N)	8900 (min)	12800	11450	11600
	Marshall Flow (0.25 mm) @ 3.5% Air Voids	8.0 (min)	8.3	8.9	9.6
	VMA %	13.5	12.8	13.57	13.3
		SuperPave Specifications			
SP 1 <i>Binder Course</i>	% of binder content @ 4.0% air voids	3 - 5	4.4	4.4	
	VMA %	14 (min)	15.7	15.5	
	VFA %	65 - 75	74.6	74.5	
	%G _{mm} @ N _{ini}	< 90.0	89.5	89.5	
	%G _{mm} @ N _{des}	< 98.0	95.5	95.0	
	P _{0.075} / P _{be} Ratio	0.6 - 1.4	1.11	1.11	
SP 2 <i>Surface Course</i>	% of binder content @ 4.0% air voids	3 - 5	4.4	4.5	4.5
	VMA %	14 (min)	14.7	12.8	14.5
	VFA %	65 - 75	73.8	70.0	73.7
	%G _{mm} @ N _{ini}	< 90.0	89.0	89.0	90.5
	%G _{mm} @ N _{des}	< 98.0	96.7	96.5	97.0
	P _{0.075} / P _{be} Ratio	0.6 - 1.4	1.11	1.11	1.11

TABLE 2 Number of Loading Cycles

Loading Frequency (Hz)	Required Number of Cycles		
	NRCC WI # 440500-9328-4.91-UIR85		AASHTO TP62-03
	Temperature (°C)		Independent of Temperature
	-10, 0	20, 30 & 40	
25	1000	700	200
10	500	300	200
5	250	150	100
1	150	60	20
0.5	50	10	15
0.1	10	10	15

TABLE 3 Stresses (kPa) Corresponding to 100 $\mu\epsilon$

Test Temperature °C	Loading Frequency (Hz)	HMA 3-58-22	HMA 3-64-34	HMA 3-52-34	HMA 1-58-22	HMA 1-52-34	SP 1-52-34	SP 1-58-22	SP 2-64-34	SP 2-58-22	SP 2-52-34
-10	20	2605	1651	1518	1575	1732	1825	2224	1874	1864	2231
	10	2614	1488	1354	1473	1670	1661	2187	1765	1772	2287
	5	2644	1379	1186	1336	1607	1519	2048	1589	1641	2135
	1	2429	1238	959	1264	1421	1274	2022	1439	1533	2110
	0.3	2329	971	789	1218	1171	1045	1911	1289	1425	1878
	0.1	2143	758	649	1133	903	837	1763	1146	1302	1620
0	20	2326	935	990	1204	976	1029	1853	1398	1530	1583
	10	2225	797	895	1097	848	870	1748	1261	1418	1442
	5	2106	724	789	1007	746	743	1624	920	1293	1268
	1	1767	518	574	913	519	493	1433	761	1124	936
	0.3	1555	388	430	838	369	335	1236	630	980	667
	0.1	1310	289	316	753	258	235	1040	476	834	476
10	20	1624		441	934						
	10	1557		351	822						
	5	1428		282	728						
	1	1084		174	573						
	0.3	815		118	461						
	0.1	556		82	362						
20	20		213			200	163	738	517	710	324
	10		164			154	118	603	414	581	239
	5		137			121	90	497	343	492	186
	1		74			69	46	303	224	320	104
	0.3		48			48	26	197	166	220	66
	0.1		34			39	16	131	130	152	45
30	20	378	87	91	298	68	83	381	219	358	142
	10	278	64	63	225	51	59	289	166	270	105
	5	205	51	45	175	40	43	226	131	210	80
	1	104	27	23	98	26	21	125	80	117	43
	0.3	63	18	14	64	22	13	81	58	72	28
	0.1	41	13	9	45	21	9	56	46	46	19
40	20	142	42	31	99	41	41	160	91	165	55
	10	99	30	20	73	36	28	118	71	123	39
	5	72	24	14	56	31	20	88	57	92	29
	1	35	13	7	32	27	10	48	39	49	16
	0.3	22	9	7	24	26	6	32	30	31	11
	0.1	17	7	3	20	25	4	24	25	22	8

TABLE 4 Typical Strain Amplitude Produced by “TableCurve”

		Parameters	Values
Equation	[Sine] $y = a + b \sin(2\pi x/d + c)$	a_2	1.91E-06
Eqn #	8014	b_2	9.87E-05 (strain amplitude, mm/mm)
R^2	0.999	c_2	3.66 (phase lag, radians)
DF Adj R^2	0.999	d_2	0.05
Fit Std Err	2.17E-06		
F-stat	105573		
Date	Dec 8, 2004		
Time	12:53:47 PM		

TABLE 5 Dynamic Modulus (MPa) and Phase Angle (°) Determined at Different Loading Frequencies and Test Temperatures for HMA1 Mix (PG 58-22)

Frequency [Hz]	Temperature [°C]									
	-10		0		20		30		40	
	E*	φ	E*	φ	E*	φ	E*	φ	E*	φ
20	13300	3.3	10000	7.6	7850	12.3	2480	34.0	825	43.0
10	12900	3.5	9540	7.7	6970	13.5	1890	36.8	608	42.6
5	11900	4.3	8830	8.7	6220	15.6	1460	38.3	467	40.7
1	11000	5.8	7940	10.1	4820	20.1	817	40.4	269	36.4
0.3	10300	6.6	7040	13.1	3840	23.8	533	40.8	200	31.4
0.1	9600	9.5	6280	16.2	3070	27.5	375	37.6	167	26.5

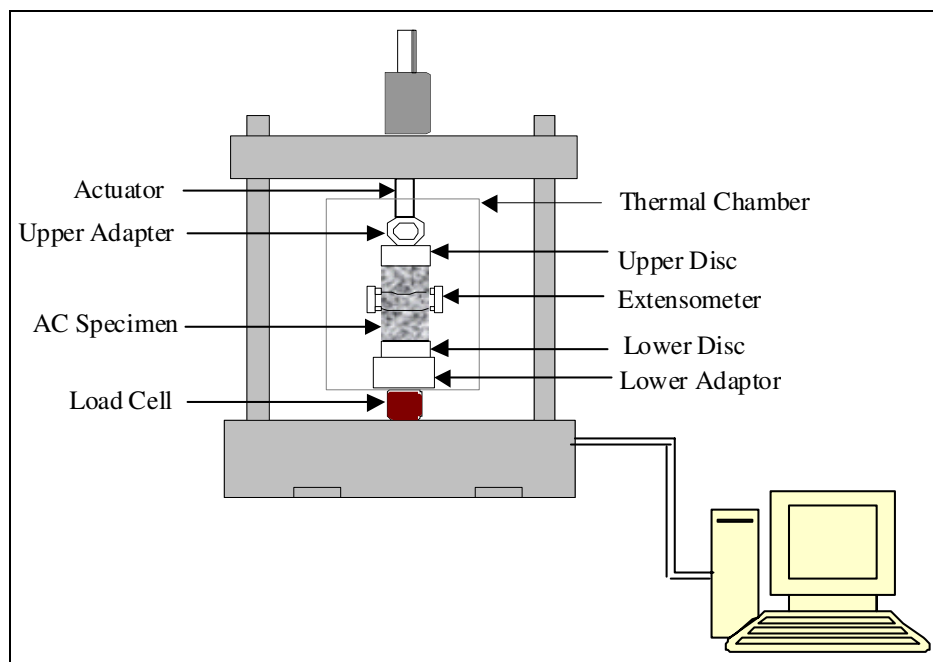
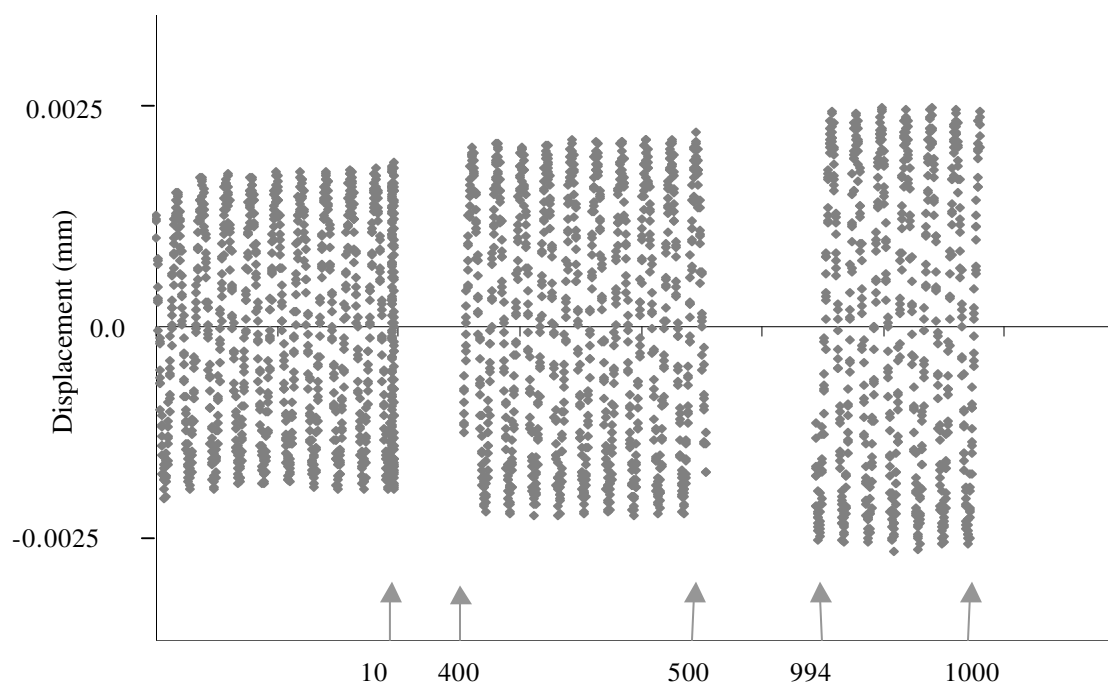
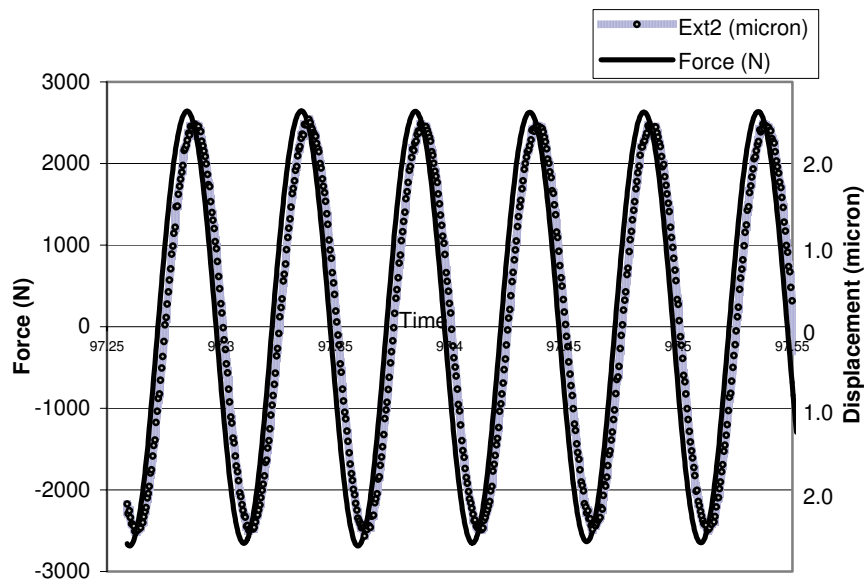


FIGURE 1 Strain-controlled test setup.



(a) Cycles needed to achieve compliance with input strain



(b) Typical real-time record of force and displacement signals

FIGURE 2 Output of the strain-controlled test.

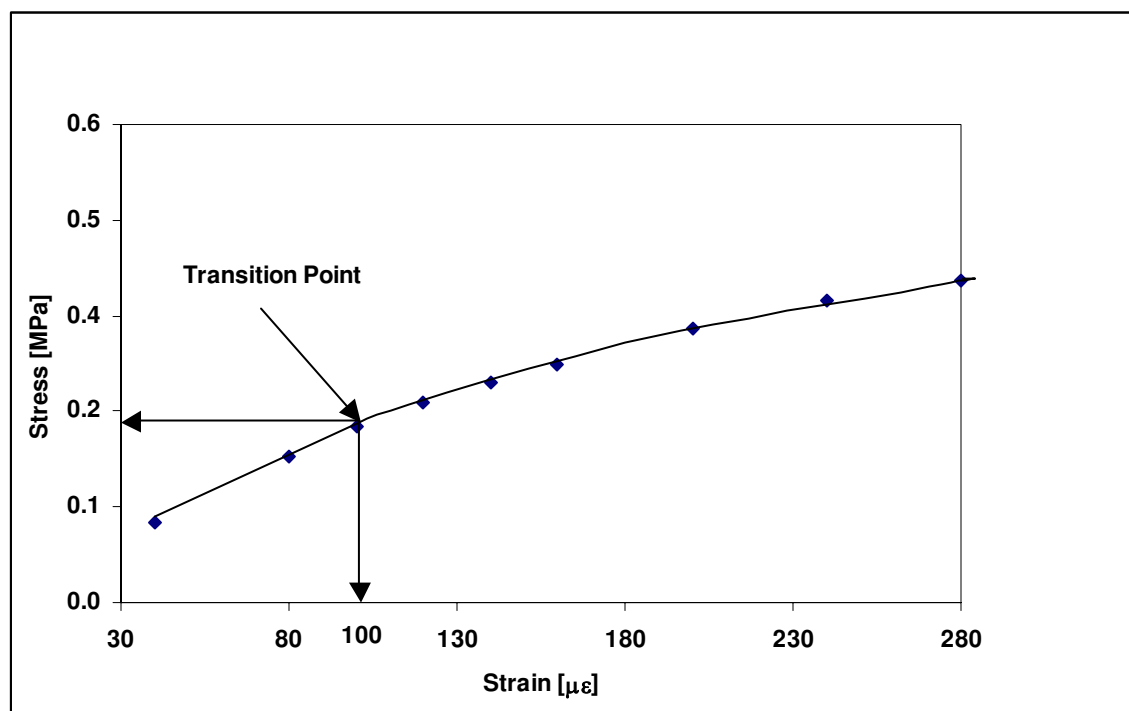


FIGURE 3 Typical stress-strain relationship at a temperature of 25°C and loading frequency of 20 Hz for SP 2 (PG 52-34).

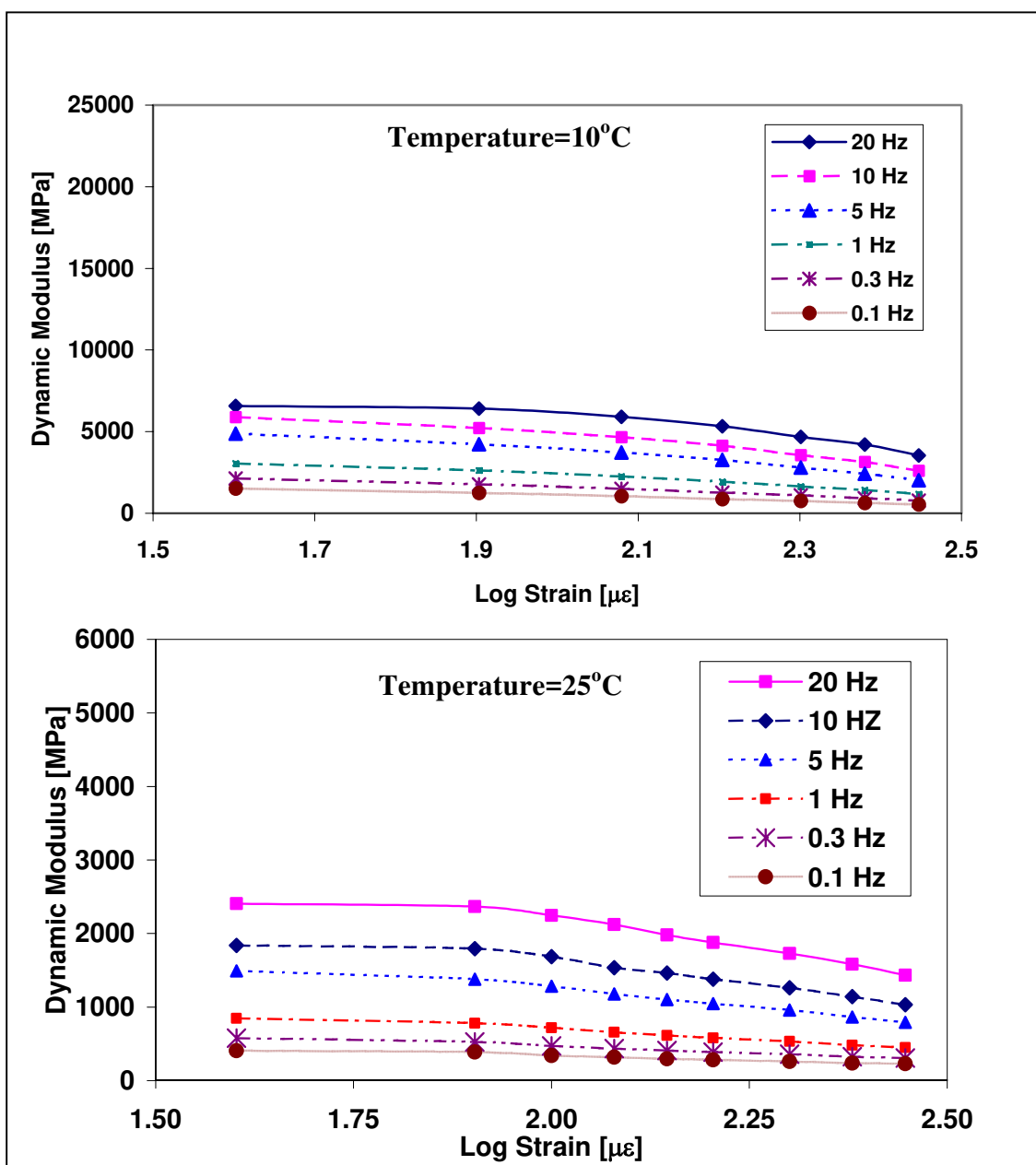


FIGURE 4 Results of a typical linearity check for tests performed at 10°C and 25°C on HMA 2 (PG 64-34).

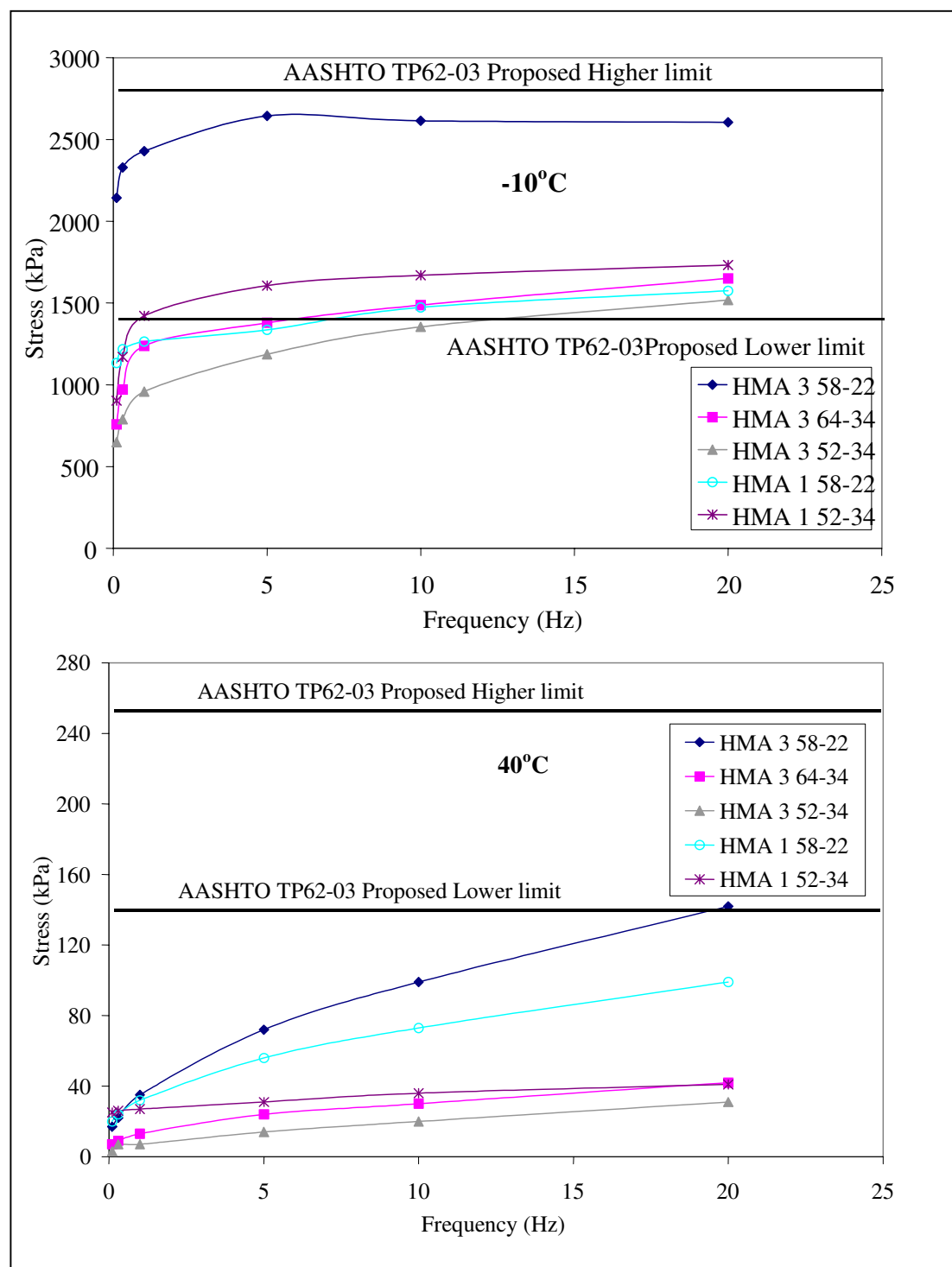


FIGURE 5 Stresses corresponding to 100 $\mu\epsilon$ for tests performed at -10 °C and 40 °C.

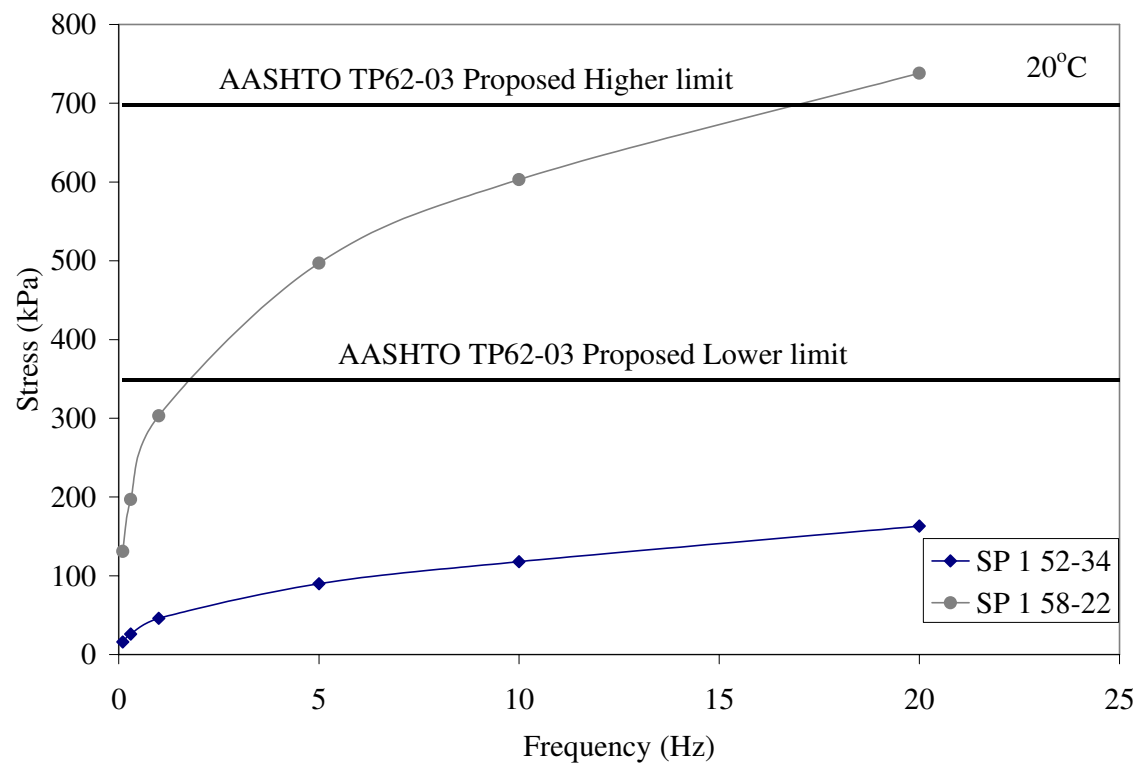


FIGURE 6 Stresses corresponding to $100\mu\epsilon$ for tests performed at 20 °C.

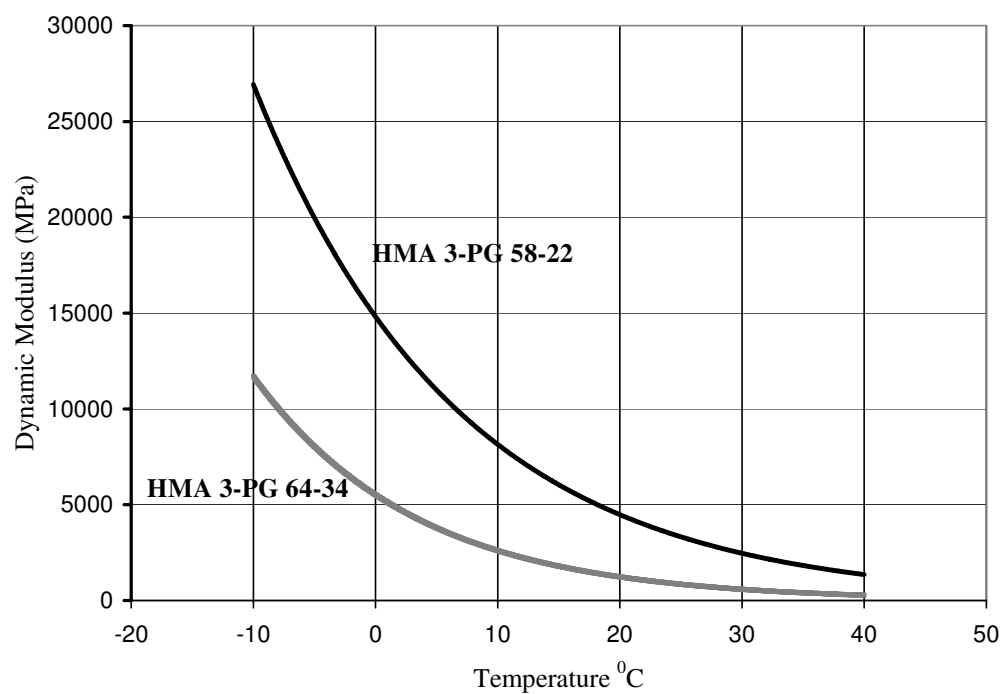


FIGURE 7 Dynamic modulus determined for HMA 3 reflecting the impact of binder type.

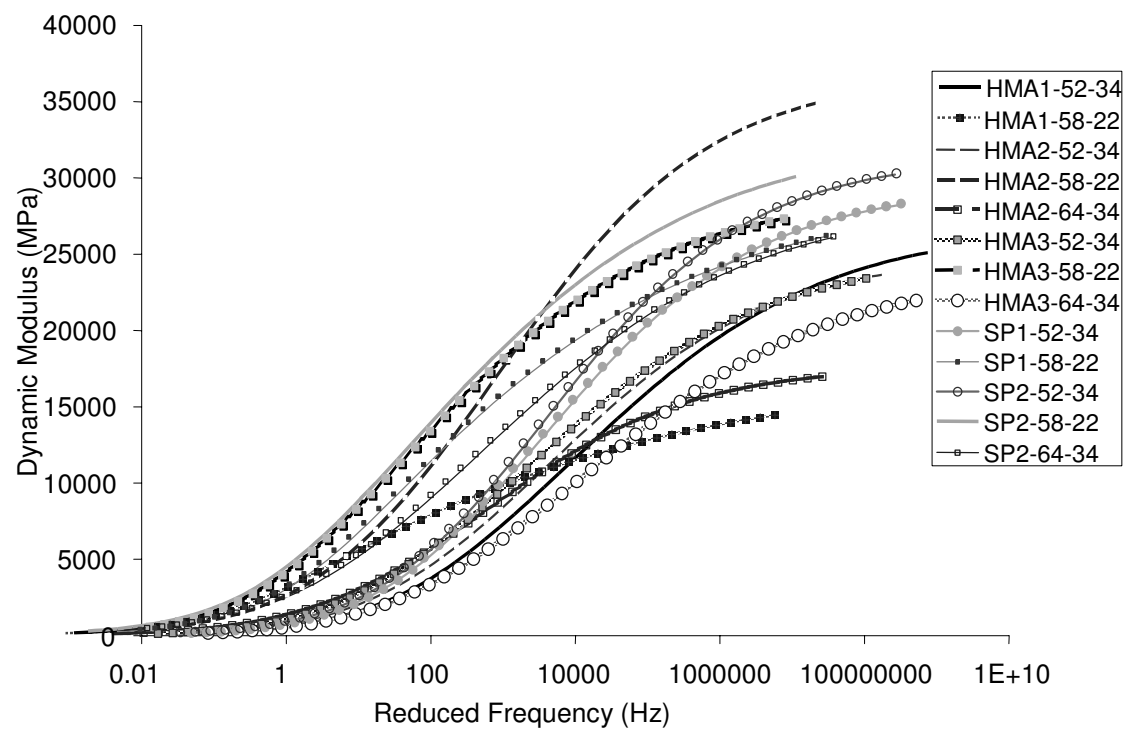


FIGURE 8 Master curves established for all mixes investigated in this study.